American Mineralogist, Volume 95, pages 1–10, 2010

Metamorphic ultrahigh-pressure tourmaline: Structure, chemistry, and correlations to *P-T* conditions

Andreas Ertl,[1,*] Horst R. Marschall,[2] Gerald Giester,[1] Darrell J. Henry,[3] Hans-Peter Schertl,[4] Theodoros Ntaflos,[5] George L. Luvizotto,[6] Lutz Nasdala,[1] and Ekkehart Tillmanns[1]

[1]Institut für Mineralogie und Kristallographie, Geozentrum, Universität Wien, Althanstrasse 14, 1090 Wien, Austria
[2]Department of Earth Sciences, Wills Memorial Building, Queen's Road, University of Bristol, Bristol BS8 1RJ, U.K.
[3]Department of Geology and Geophysics, Louisiana State University, Baton Rouge, Louisiana 70803, U.S.A.
[4]Institut für Geologie, Mineralogie und Geophysik, Ruhr-Universität Bochum, D-44780 Bochum, Germany
[5]Department für Lithosphärenforschung, Geozentrum, Universität Wien, Althanstrasse 14, A-1090 Wien, Austria
[6]Institut für Geowissenschaften, Universität Heidelberg, Im Neuenheimer Feld 236, D-69120 Heidelberg, Germany

Abstract

Tourmaline grains extracted from rocks within three ultrahigh-pressure (UHP) metamorphic localities have been subjected to a structurally and chemically detailed analysis to test for any systematic behavior related to temperature and pressure. Dravite from Parigi, Dora Maira, Western Alps (peak *P-T* conditions ~3.7 GPa, 750 °C), has a structural formula of $^{X}(Na_{0.90}Ca_{0.05}K_{0.01}\square_{0.04})$ $^{Y}(Mg_{1.78}Al_{0.99}Fe^{2+}_{0.12}Ti^{4+}_{0.03}\square_{0.08})^{Z}(Al_{5.10}Mg_{0.90})(BO_3)_3{}^{T}Si_{6.00}O_{18}{}^{V}(OH)_3{}^{W}[(OH)_{0.72}F_{0.28}]$. Dravite from Lago di Cignana, Western Alps, Italy (~2.7–2.9 GPa, 600–630 °C), has a formula of $^{X}(Na_{0.84}Ca_{0.09}K_{0.01}\square_{0.06})$ $^{Y}(Mg_{1.64}Al_{0.79}Fe^{2+}_{0.48}Mn^{2+}_{0.06}Ti^{4+}_{0.02}Ni_{0.02}Zn_{0.01})^{Z}(Al_{5.00}Mg_{1.00})(BO_3)_3{}^{T}(Si_{5.98}Al_{0.02})O_{18}{}^{V}(OH)_3{}^{W}[(OH)_{0.65}F_{0.35}]$. "Oxy-schorl" from the Saxonian Erzgebirge, Germany (≥4.5 GPa, 1000 °C), most likely formed during exhumation at >2.9 GPa, 870 °C, has a formula of $^{X}(Na_{0.86}Ca_{0.02}K_{0.02}\square_{0.10})^{Y}(Al_{1.63}Fe^{2+}_{1.23}Ti^{4+}_{0.11}Mg_{0.03}Zn_{0.01})$ $^{Z}(Al_{5.05}Mg_{0.95})(BO_3)_3{}^{T}(Si_{5.96}Al_{0.04})O_{18}{}^{V}(OH)_3{}^{W}[O_{0.81}F_{0.10}(OH)_{0.09}]$. There is no structural evidence for significant substitution of $^{[4]}$Si by $^{[4]}$Al or $^{[4]}$B in the UHP tourmaline (<T-O> distances ~1.620 Å), even in high-temperature tourmaline from the Erzgebirge. This is in contrast to high-*T*–low-*P* tourmaline, which typically has significant amounts of $^{[4]}$Al. There is an excellent positive correlation ($r^2 = 1.00$) between total $^{[6]}$Al (i.e., ^{Y}Al + ^{Z}Al) and the determined temperature conditions of tourmaline formation from the different localities. Additionally, there is a negative correlation ($r^2 = 0.97$) between F content and the temperature conditions of UHP tourmaline formation and between F and ^{Y}Al content ($r^2 = 1.00$) that is best explained by the exchange vector $^{Y}AlO(R^{2+}F)_{-1}$. This is consistent with the W site (occupied either by F, O, or OH), being part of the YO_6-polyhedron. Hence, the observed Al-Mg disorder between the Y and Z sites is possibly indirectly dependent on the crystallization temperature.

Keywords: Tourmaline, ultrahigh pressure, Saxonian Erzgebirge, Western Alps, Dora Maira, Lago di Cignana

Introduction and previous work

Tourmaline can be formed in different geochemical environments that have undergone magmatic, metasomatic, diagenetic, or metamorphic processes (Henry and Guidotti 1985; Deer et al. 1992; Henry and Dutrow 1992, 1996; Slack 1996; Dutrow et al. 1999; Henry et al. 1999, 2008; Bernardelli et al. 2000; Kawakami 2001; Sengupta et al. 2005; van den Bleeken et al. 2007; Ertl et al. 2008b; Trumbull et al. 2008; Marschall et al. 2009). The general chemical formula of the tourmaline-group minerals is given as $XY_3Z_6[T_6O_{18}](BO_3)_3V_3W$ by Hawthorne and Henry (1999). The X site is usually occupied by Na, Ca, and rarely by K, but can also be vacant. Fe^{2+}, Fe^{3+}, Mn^{2+}, Mg, Li, Cu, Ti^{4+}, V^{3+}, and Cr^{3+} typically occupy the Y site, which is often also characterized by significant amounts (>5% of the site occupancy) of Al. The Z site is usually occupied by Al, but in some cases, contains significant amounts of Mg, Fe^{3+}, and, more rarely, V^{3+} and Cr^{3+}. The replacement of Al by Mg at the Z site was described by Grice and Ercit (1993), Hawthorne et al. (1993), Bloodaxe et al. (1999), Ertl et al. (2003a, 2008a), Bosi and Lucchesi (2004), Bosi et al. (2004), and Marschall et al. (2004). The T site is usually occupied by Si, but can also incorporate significant amounts of Al (Foit and Rosenberg 1979; MacDonald and Hawthorne 1995) and B (Ertl et al. 1997, 2008b, and references therein).

Tourmaline compositions in metamorphic rocks are strongly related to the local bulk composition and mineral assemblages, but there are some general trends that are apparently a function of metamorphic grade. Based on a survey of natural tourmaline data, Henry and Dutrow (1996) suggested that, at increasing metamorphic grade, there is an increase in tetrahedral Al via the $Al_2(R^{2+}Si)_{-1}$ exchange vector, an increase in F contents at the W site, and a decrease of X-site vacancies via the $^{X}\square Al(NaR^{2+})_{-1}$ exchange vector (where $R^{2+} = Fe^{2+}$, Mn^{2+}, Mg). In contrast, the experimental study of van Goerne et al. (2001) suggested that for a fixed Na content in the fluid phase, the latter exchange

* E-mail: andreas.ertl@a1.net

vector increases with temperature. A further trend observed in natural tourmaline is an increase in Ti as a function of increasing temperature (Thomson 2006). Perhaps the most distinctive temperature-sensitive tourmaline compositional feature is its compositional polarity (sector zoning) such that tourmaline develops significantly different compositions at the opposite poles of the *c*-axis of the tourmaline (Henry and Dutrow 1996; van Hinsberg and Schumacher 2007; van Hinsberg and Marschall 2007). The compositional polarity decreases as a function of temperature and disappears at medium grades of metamorphism and has been suggested as a geothermometer (Henry and Dutrow 1996; van Hinsberg and Schumacher 2007).

Tourmaline stability

Tourmaline is stable over a wide pressure-temperature (*P-T*) interval (Marschall et al. 2009, and references therein). It ranges from diagenetic/epigenetic through high-grade metamorphic conditions and up to magmatic conditions (e.g., ~150–850 °C at ~0.1–0.4 GPa; Robbins and Yoder 1962; Manning and Pichavant 1983). The stability of dravite was established in experiments by Werding and Schreyer (2002) to lie between pressures of 3–5 GPa and temperatures >950 °C (Fig. 1). The breakdown of dravite to different Al-Mg phases occurs at pressures as high as 6–8 GPa (Krosse 1995). In the presence of coesite, natural tourmaline breaks down at pressures exceeding 4 GPa in the temperature range of 800–850 °C and at 4.5–5 GPa at lower temperatures of about 700 °C (Fig. 1) (Ota et al. 2008).

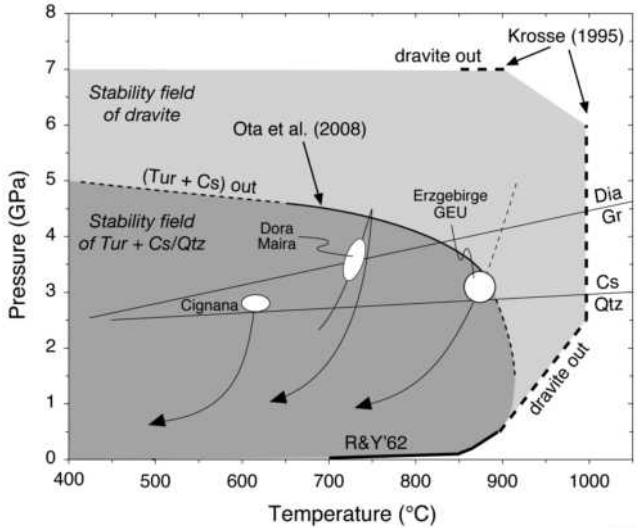

Figure 1. *P-T* diagram showing: (1) the experimentally determined stability field of dravitic tourmaline (light gray) (Robbins and Yoder 1962; Krosse 1995; Werding and Schreyer 2002) and tourmaline + coesite/quartz (dark gray) (Ota et al. 2008), and (2) peak metamorphic conditions of the different tourmaline-bearing UHP rocks investigated (white ellipses): Diamond- and coesite-bearing gneisses from the gneiss-eclogite unit (GEU) of the Saxonian Erzgebirge, Germany (Schmädicke and Müller 2000; Massonne 2003; Massonne et al. 2007); coesite-pyrope-kyanite quartzite from the Dora Maira massif, Western Alps, Italy (Schreyer 1985; Schertl et al. 1991); coesite-bearing metasediments from Lago di Cignana, Western Alps, Italy (Reinecke 1991, 1998; Bebout and Nakamura 2003). Quartz-coesite and graphite-diamond equilibria after Bohlen and Boettcher (1982) and Bundy (1980), respectively.

Regional geology of the ultrahigh-pressure (UHP) massifs and sample characteristics

In the present study, three different natural tourmaline samples were investigated, all of which formed under ultrahigh-pressure (UHP) metamorphic conditions. One tourmaline sample studied (dravite, no. 15597) comes from a pyrope quartzite from Parigi, Dora Maira Massif, Western Alps, Italy (Chopin 1984). Peak metamorphic conditions were estimated at ~3.5 GPa and 750 °C (Chopin 1984; Schertl et al. 1991; Compagnoni 2003), or possibly at higher pressures within the diamond stability field (Hermann 2003). Quartz pseudomorphs after coesite and tourmaline grains are present as inclusions within pure pyrope (Fig. 2a). According to Schreyer (1985), who investigated the same sample, pyrope replaced a preexisting fabric of oriented tourmaline crystals leading to a poikiloblastic texture (Schreyer 1985, their Fig. 14). Several similarly oriented inclusions of dravite in pyrope were taken as evidence for the growth of pyrope and kyanite at the expense of tourmaline (Schreyer 1985; Schertl et al. 1991). Experimental work by Hermann (2003) revealed that peak conditions of the pyrope quartzite were 4.5 GPa and 750 °C. Interestingly, these conditions are very similar to where the reaction Tur + Cs = Grt + Cpx + Ky + fluid was located experimentally (Ota et al. 2008) (most mineral abbreviations after Kretz 1983). This suggests that the tourmaline in the Dora Maira pyrope quartzite survived diamond facies conditions as monomineralic inclusions in garnet and kyanite, but was decomposed to garnet + kyanite + fluid where in contact with coesite. The Mg-rich quartzites are interpreted as strongly metasomatized equivalents of the surrounding granitic gneisses (Schertl and Schreyer 2008). Hence, the Dora-Maira dravite may have formed during the same metasomatic event. The quartz-bearing (former coesite; Fig. 2a) assemblage confirms that the host pyrope formed as a result of the reaction talc + kyanite = pyrope + coesite (second pyrope-forming reaction; Schertl et al. 1991) near peak metamorphic conditions. Thus, the host pyrope is not a "large pyrope" that may exceed 15 cm in diameter (larger pyrope grains formed along the prograde *P-T* path due to the first pyrope forming reaction chlorite + kyanite + talc = pyrope; Schertl et al. 1991) as suggested by Schreyer (1985) in his first exploratory study of this sample.

The second location of UHP rocks from which Mg-rich tourmaline was studied is near Lago di Cignana in the Western Alps (Reinecke 1991, 1998; Bebout and Nakamura 2003). The sample is a metasedimentary piemontite- and talc-bearing garnet-phengite-coesite-schist; *P-T* conditions have been estimated as ~2.7–2.9 GPa and ~600–630 °C (Reinecke 1991, 1998). Reinecke (1991) described inclusions of relict coesite, hematite, rutile, and braunite in tourmaline grains from this locality.

A third UHP tourmaline-bearing locality is located in the Erzgebirge at the northwestern margin of the Bohemian Massif, which is part of the Devonian-Carboniferous metamorphic basement of the Mid-European Variscides exposed in Saxony and the northern Czech Republic. The region is characterized by a stack of five tectono-metamorphic units, each with distinct *P-T* histories (Willner et al. 1997; Rötzler et al. 1998). The investigated sample (R6b) is from the diamond- and coesite-bearing gneiss-eclogite unit (GEU); *P-T* estimates of the eclogite revealed

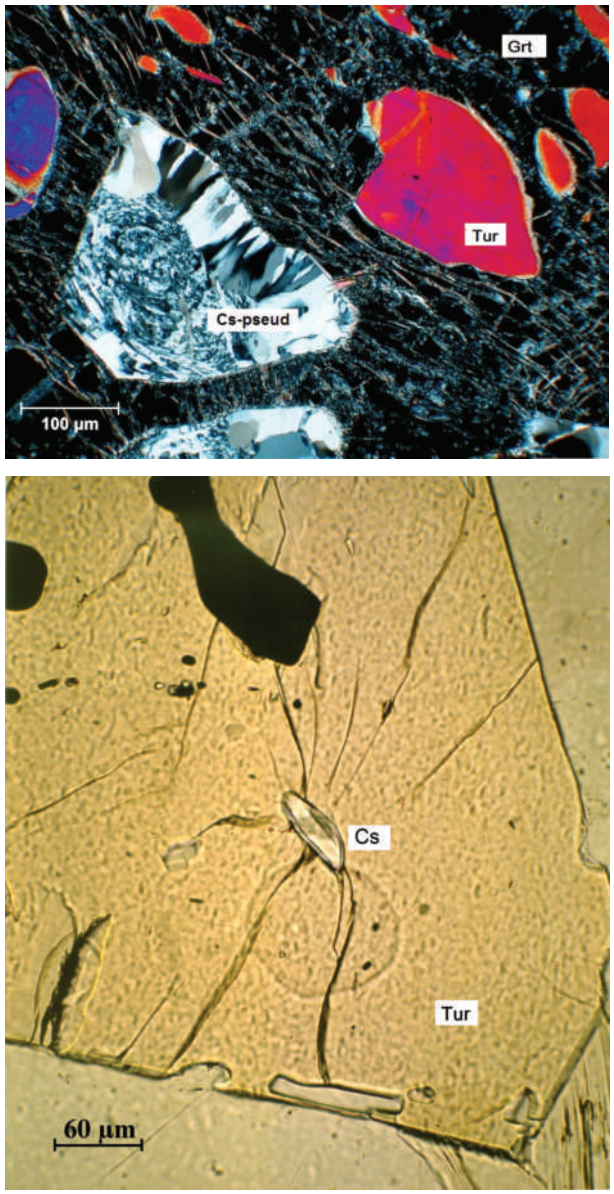

FIGURE 2. (**a**) Quartz-pseudomorph after coesite (Cs-pseud) and tourmaline (Tur) inclusions in pyrope from Dora Maira, Western Alps, Italy. (**b**) Relic coesite inclusion (confirmed by Raman spectroscopy; Reinecke 1991) in a euhedral tourmaline crystal from Lago di Cignana, Western Alps, Italy.

conditions of >2.9 GPa at 870 °C (Schmädicke and Müller 2000), but the occurrence of diamond in the felsic gneisses requires pressures in excess of 4 GPa (Massonne 2003; Massonne et al. 2007). Peak metamorphic conditions may have been even higher (8 GPa at >1050 °C; Massonne 2003). The sample was collected as a loose decimeter-sized block from a small creek 5 km ENE of the Saidenbach reservoir, Forchheim, Pockau, Erzgebirge, Saxony, Germany. It is a felsic, medium-grained, granulite-facies mylonite displaying strongly elongated quartz and feldspar with black tourmaline porphyroclasts and minor garnet. Short, prismatic tourmaline crystals are up to 3 mm in length. In thin section (cut perpendicular to the *c*-axis), the tourmaline crystals show three distinct color zones separated by diffuse boundaries: a blue core, a brownish mantle, and a greenish-gray anhedral rim, the latter of which is intimately intergrown with quartz, feldspar, and phengite in the matrix. Marschall et al. (2009) noted coesite and kyanite inclusions in the mantle zone of tourmaline from Erzgebirge (in sample R6b). A fourth tourmaline sample was available from an UHP gneiss from the Kokchetav Massif, Kazakhstan (Dobretsov et al. 1995), but was not considered because its development under UHP conditions has been questioned (Marschall et al. 2009).

EXPERIMENTAL DETAILS

Sample selection and preparation

Reddish tourmaline crystals were hand picked under the microscope from a crushed piece (~5 cm) of the piemontite- and talc-bearing garnet-phengite-coesite-schist (investigated by Reinecke 1998) from Lago di Cignana. After optical inspection, the clearest fragment (sample Laci; ~0.15 × 0.20 × 0.24 mm) was used for single-crystal structure refinements and subsequently for chemical analyses. Similar tourmaline grains from this locality contain coesite inclusions (Reinecke 1991; see also Fig. 2b). The tourmaline fragment from the Dora Maira locality (sample Domai; 0.12 × 0.15 × 0.25 mm) was extracted from a thin section, where it forms anhedral inclusions in a relatively small pyrope crystal (~1 cm) (see Schreyer 1985, Fig. 14 therein). The host pyrope of this tourmaline inclusion also contains quartz pseudomorphs after coesite (Fig. 2a). The fragment from Erzgebirge (sample R6b; 0.15 × 0.22 × 0.22 mm) was broken off from the coesite-bearing mantle (Marschall et al. 2009) of a macroscopically black tourmaline crystal. For electron microprobe analyses (EMPA), samples were embedded in araldite epoxy, and flat polished sample mounts were produced.

All UHP tourmaline crystals investigated contain inclusions, which were identified by Raman spectroscopy (data not presented here) and electron microprobe analysis (EMPA). In the sample from Dora Maira a phengite inclusion (~2 µm in diameter) was observed. In the tourmaline from Lago di Cignana, talc (~12 µm in length), zircon (a crystal with ~3 µm in diameter), and a mineral of the epidote group (~15 µm in diameter) with the composition $(Ca_{1.75}Mn^{2+}_{0.25})(Al_{2.02}Mn^{3+}_{0.49}Fe^{3+}_{0.49})(SiO_4)(Si_2O_7)(O,OH)_2$ were identified. This epidote-group mineral belongs to the piemontite-epidote series with a sursassite component of ~13 mol% (similar to the chemical data of piemontite from the matrix of the rock as described by Reinecke 1991). A kyanite inclusion (~3 µm in length) was observed the tourmaline sample from Erzgebirge.

Crystal structure refinement

Tourmaline samples were examined on a Kappa APEX II CCD X-ray single-crystal diffractometer from Bruker AXS equipped with a monocapillary optics collimeter, graphite-monochromatic Mo$K\alpha$ radiation (Universität Wien). Data were collected at room temperature with sixfold redundancy (up to 80 °2θ), and integrated and corrected for Lorentz and polarization factors (Bruker 2001). Absorption correction by evaluation of multiple scans was applied. The structure was refined with SHELXL-97 (Sheldrick 1997) using scattering factors for neutral atoms and a tourmaline starting model from Ertl et al. (2006). Table 1 provides crystal data and details of the structure refinement. Table 2 provides atomic parameters (anisotropic displacement parameters are available upon request or from the MSA American Mineralogist Crystal Structure Database, http://www.minsocam.org/MSA/Crystal_Database.html), and Table 3 provides selected interatomic distances. The H atom bonded to the O3 atom was located from a difference-Fourier map and subsequently refined. Refinement was performed with anisotropic thermal parameters for all non-hydrogen atoms. Site occupancies were refined according to well-known characteristics of the tourmaline structure (Na was refined at the X site; Mg and Fe were refined at the Y site; for other details see Table 2; the correlation coefficients do not show significant correlations in the refinement, e.g., between site occupancy and overall scale factor). The refinement converged at $R1(F)$ values of 1.3–2.0%.

Electron microprobe analyses

The three single crystals that were used for the crystal-structure determination were subsequently analyzed with a CAMECA SX-100 electron microprobe at the Department of Lithospheric Research, Geozentrum, Universität Wien, Austria, equipped with four wavelength-dispersive spectrometers (Table 4).

TABLE 1. Crystallographic data and refinement details for UHP tourmaline samples

Sample	R6b	Domai	Laci
a, *c* (Å)	15.929(1), 7.183(1)	15.935(1), 7.201(1)	15.945(1), 7.210(1)
V (Å^3)	1578.4(4)	1583.5(4)	1587.5(4)
Crystal dimensions (mm)	0.15 × 0.22 × 0.22	0.12 × 0.15 × 0.25	0.15 × 0.20 × 0.24
Collection mode, $2\theta_{max}$ (°)	full sphere, 91.40	full sphere, 90.78	full sphere, 87.93
h, *k*, *l* ranges	–31/32, –30/31, –13/14	–31/30, –30/31, –14/13	–31/31, –31/30, –13/13
Total reflections measured	43951	42893	43361
Unique reflections	3139 (R_{int} 1.86%)	3026 (R_{int} 2.93%)	2935 (R_{int} 2.09%)
$R_1(F)$, $wR_2(F^2)$	1.31%, 3.55%	2.01%, 4.41%	1.36%, 3.45%
Flack *x* parameter	0.058(21)	0.053(48)	0.040(18)
"Observed" refls. [$F_o > 4\sigma_{(Fo)}$]	3098	2803	2884
Extinct. coefficient	0.00371(15)	0.00371(13)	0.00371(12)
No. of refined parameters	95	95	95
GooF	0.831	0.949	0.819
$\Delta\sigma_{min}$, $\Delta\sigma_{max}$ (e/Å^3)	–0.36, 0.47	–0.41, 0.49	–0.28, 0.36

Note: R6b = Erzgebirge; Domai = Dora Maira; Laci = Lago di Cignana.

TABLE 2. Table of atom parameters in UHP tourmaline samples

Site	Sample	*x*	*y*	*z*	U_{eq}	*Occ.*
X	R6b	0	0	0.2250(2)	0.0219(3)	$Na_{0.91(1)}$
	Domai	0	0	0.2396(2)	0.0214(3)	$Na_{1.02(1)}$
	Laci	0	0	0.2325(1)	0.0204(2)	$Na_{1.00(1)}$
Y	R6b	0.12241(1)	1/2×	0.63418(3)	0.00765(4)	$Mg_{0.609(1)}Fe_{0.391}$
	Domai	0.12571(3)	1/2×	0.63044(5)	0.0081(2)	$Mg_{0.933(1)}Fe_{0.067}$
	Laci	0.12426(2)	1/2×	0.63250(3)	0.00810(6)	$Mg_{0.808(1)}Fe_{0.192}$
Z	R6b	0.29781(1)	0.26128(1)	0.60853(2)	0.00541(4)	$Al_{1.00}$
	Domai	0.29806(2)	0.26164(2)	0.61163(3)	0.00622(4)	$Al_{1.00}$
	Laci	0.29802(1)	0.26159(1)	0.61070(2)	0.00545(3)	$Al_{1.00}$
B	R6b	0.10999(3)	2×	0.4526(1)	0.0068(1)	$B_{1.00}$
	Domai	0.10979(4)	2×	0.4546(2)	0.0069(1)	$B_{1.00}$
	Laci	0.10987(3)	2×	0.4536(1)	0.0065(2)	$B_{1.00}$
T	R6b	0.19157(1)	0.18968(1)	–0.00115(2)	0.00525(3)	$Si_{1.00}$
	Domai	0.19191(1)	0.19000(1)	–0.00089(3)	0.00548(3)	$Si_{1.00}$
	Laci	0.19175(1)	0.18990(1)	–0.00135(2)	0.00520(3)	$Si_{1.00}$
H3	R6b	0.252(2)	1/2×	0.397(4)	0.042(7)	$H_{1.00}$
	Domai	0.259(2)	1/2×	0.400(4)	0.049(9)	$H_{1.00}$
	Laci	0.256(2)	1/2×	0.400(3)	0.045(7)	$H_{1.00}$
O1	R6b	0	0	0.7708(2)	0.0224(4)	$O_{0.81(1)}F_{0.19}$
	Domai	0	0	0.7720(2)	0.0144(4)	$O_{0.68(1)}F_{0.32}$
	Laci	0	0	0.7712(2)	0.0135(2)	$O_{0.61(1)}F_{0.39}$
O2	R6b	0.06101(2)	2×	0.48628(9)	0.0130(1)	$O_{1.00}$
	Domai	0.06094(3)	2×	0.4848(1)	0.0111(1)	$O_{1.00}$
	Laci	0.06106(2)	2×	0.48347(9)	0.01023(9)	$O_{1.00}$
O3	R6b	0.26269(7)	1/2×	0.50873(9)	0.0158(1)	$O_{1.00}$
	Domai	0.26529(8)	1/2×	0.5106(1)	0.0127(1)	$O_{1.00}$
	Laci	0.26510(6)	1/2×	0.50989(9)	0.0125(1)	$O_{1.00}$
O4	R6b	0.09338(3)	2×	0.07027(9)	0.01067(9)	$O_{1.00}$
	Domai	0.09305(3)	2×	0.0694(1)	0.0107(1)	$O_{1.00}$
	Laci	0.09310(3)	2×	0.06931(9)	0.01017(9)	$O_{1.00}$
O5	R6b	0.18558(5)	1/2×	0.09176(9)	0.01051(9)	$O_{1.00}$
	Domai	0.18401(7)	1/2×	0.0909(1)	0.0106(1)	$O_{1.00}$
	Laci	0.18433(5)	1/2×	0.09025(9)	0.01010(9)	$O_{1.00}$
O6	R6b	0.19525(3)	0.18501(3)	0.77532(6)	0.00927(6)	$O_{1.00}$
	Domai	0.19604(4)	0.18586(4)	0.77669(8)	0.00877(8)	$O_{1.00}$
	Laci	0.19581(3)	0.18592(3)	0.77662(6)	0.00840(6)	$O_{1.00}$
O7	R6b	0.28521(3)	0.28528(3)	0.07611(6)	0.00885(6)	$O_{1.00}$
	Domai	0.28501(4)	0.28490(4)	0.07900(8)	0.00867(8)	$O_{1.00}$
	Laci	0.28489(3)	0.28483(3)	0.07811(6)	0.00850(6)	$O_{1.00}$
O8	R6b	0.20931(3)	0.27011(3)	0.43816(7)	0.01020(6)	$O_{1.00}$
	Domai	0.20952(4)	0.27018(4)	0.44103(8)	0.00961(8)	$O_{1.00}$
	Laci	0.20927(3)	0.27006(3)	0.44018(6)	0.00962(6)	$O_{1.00}$

Notes: R6b = Erzgebirge; Domai = Dora Maira; Laci = Lago di Cignana. Definition for U_{eq} see Fischer and Tillmanns (1988).

The following (natural and synthetic) standards and X-ray lines for calibration were used: albite (Na*K*α), olivine (Mg*K*α, Si*K*α, Fe*K*α), almandine (Al*K*α), rutile (Ti*K*α), orthoclase (K*K*α), wollastonite (Ca*K*α), spessartine (Mn*K*α), gahnite (Zn*K*α), NiO (Ni*K*α), and apatite-(CaF) (F*K*α). Matrix corrections were performed using the PAP correction procedure provided in the CAMECA's latest PeakSight version 4.0 software. An accelerating voltage of 20 keV and a beam current of 20 nA were used for all elements except for F (10 keV, 20 nA). The method of peak to background ratio with counting time 20 s on peak position and 10 s on each background position were used; the beam was defocused to 5 µm in diameter. Under the conditions described, analytical errors are ±2% relative for major elements and ±5% relative for minor elements as estimated from the reproducibility observed in multiple measurements. All investigated tourmaline fragments were very homogeneous as indicated by low standard deviations of multiple analyses on single crystals (Table 4).

RESULTS

Crystal structures

The general structural formula of tourmaline is given by Hawthorne and Henry (1999) as $XY_3Z_6(BO_3)_3(T_6O_{18})V_3W$, where the V and W sites are anion sites. In the following subsections,

TABLE 3. Selected interatomic distances in UHP tourmaline samples (standard deviation in brackets)

Sample	R6b	Domai	Laci
X-			
O2 ×3	2.521(1)	2.439(1)	2.473(1)
O5 ×3	2.733(1)	2.756(1)	2.7443(8)
O4 ×3	2.8060(9)	2.846(1)	2.8278(8)
Mean	2.687(1)	2.680(1)	2.682(1)
Y-			
O1	1.9531(8)	2.0120(9)	1.9861(7)
O2 ×2	1.9929(5)	2.0051(6)	2.0122(5)
O6 ×2	1.9938(5)	2.0026(6)	2.0064(5)
O3	2.1348(9)	2.111(1)	2.1362(8)
Mean	2.0102(6)	2.0231(7)	2.0266(6)
Z-			
O6	1.8963(5)	1.8843(6)	1.8912(5)
O7	1.8987(5)	1.9031(6)	1.9055(5)
O8	1.8959(5)	1.8943(6)	1.8986(5)
O8′	1.9242(5)	1.9263(6)	1.9296(5)
O7′	1.9571(5)	1.9573(6)	1.9610(5)
O3	1.9880(4)	1.9885(5)	1.9893(4)
Mean	1.9267(5)	1.9256(6)	1.9292(5)
T-			
O7	1.6066(4)	1.6047(6)	1.6053(4)
O6	1.6097(5)	1.6057(6)	1.6046(5)
O4	1.6245(3)	1.6259(4)	1.6262(3)
O5	1.6400(3)	1.6414(4)	1.6414(3)
Mean	1.6202(4)	1.6194(5)	1.6194(4)
B-			
O2	1.373(1)	1.366(1)	1.365(1)
O8 (×2)	1.3740(6)	1.3797(8)	1.3760(6)
Mean	1.374(1)	1.375(1)	1.372(1)

we discuss the occupancy of the different sites of the studied tourmalines samples.

X-site occupancy. In all samples, the X site is occupied mainly by Na (0.84–0.90 apfu) by small amounts of Ca (0.02–0.09 apfu), and by minor amounts of K (≤0.02 apfu). X-site vacancies are between 0.04 and 0.10 apfu (Table 4).

Y-site occupancy. The Y site of the samples from Dora Maira and Lago di Cignana is predominantly occupied by Mg, but also contains significant amounts of ^{Y}Al. Only the sample from Erzgebirge contains appreciable amounts of Al (~1.6 apfu) at the Y site, as indicated by the relatively short <Y-O> distance of 2.010 Å (Table 3). The samples from Dora Maira and Lago di Cignana have larger <Y-O> distances with 2.023–2.027 Å indicative of significant amounts of (Mg+Fe^{2+}) at the Y site (Table 3). The respective amounts of divalent iron at the Y sites (0.12–1.23 apfu) of the samples investigated are given in Table 4. Although no Mössbauer spectroscopy was performed, a significant amount of Fe^{3+} in these samples is not likely; the color of tourmaline from Dora Maira (very pale brown) and from the mantle zone of Erzgbirge tourmaline (deep brown in thick section) may be explained by intervalence charge transfer of Fe^{2+}-Ti^{4+} (Rossman 2008). Only the Lago di Cignana sample contains a significant amount of Mn^{2+} (0.06 apfu). This sample may also contain some Mn^{3+}, as indicated by the reddish color (Reinitz and Rossman 1988; Ertl et al. 2003b). All samples show small amounts of Ti^{4+} (0.02–0.11 apfu). The Lago di Cignana and Erzgebirge samples show minor amounts of Zn (ZnO: 0.06–0.09 wt%; Table 4); the tourmaline from Lago di Cignana is characterized by significant amounts of Ni (NiO: 0.15 wt%; Table 4), which is not surprising because the associated minerals (phlogopite and clinochlore) from the oceanic metasediments also contain significant Ni (0.07–0.18 wt% NiO; Reinecke 1991). Nickel content is probably derived from serpentinites associated with the metasediments.

TABLE 4. Composition of UHP tourmaline samples (wt%, standard deviation in brackets)

Sample	R6b	Domai	Laci
SiO_2	35.85(9)	37.40(13)	36.80(11)
TiO_2	0.87(1)	0.21(4)	0.13(2)
B_2O_3[1]	10.46	10.85	10.70
Al_2O_3	34.32(6)	32.23(18)	30.35(17)
Cr_2O_3	0.01(1)	b. d.	0.02(1)
FeO	8.87(7)	0.91(4)	3.55(12)
MnO	0.02(1)	b. d.	0.42(14)
MgO	3.96(4)	11.21(15)	10.92(7)
ZnO	0.09(1)	b. d.	0.06(1)
NiO	b. d.	b. d.	0.15(1)
CaO	0.12(1)	0.29(3)	0.50(3)
Na_2O	2.67(5)	2.90(5)	2.68(4)
K_2O	0.08(1)	0.05(1)	0.05(1)
H_2O[2]	2.79*	3.48	3.37
F	0.20(2)	0.55(7)	0.67(9)
O≡F	–0.08	–0.23	–0.28
Sum	100.23	99.85	100.09
Si apfu	5.96	6.00	5.98
$^{[4]}$Al	0.04	–0.02	
Sum T-site	6.00	6.00	6.00
$^{[3]}$B	3.00	3.00	3.00
Al	6.68	6.09	5.79
Fe^{2+}	1.23	0.12	0.48
Mn^{2+}	–	–0.06	
Mg	0.98	2.68	2.64
Ti^{4+}	0.11	0.03	0.02
Zn	0.01	–0.01	
Ni	–	–0.02	
Sum Y-,Z-sites	9.01	8.92	9.02
Ca	0.02	0.05	0.09
Na	0.86	0.90	0.84
K	0.02	0.01	0.01
□	0.10	0.04	0.06
Sum X-site	1.00	1.00	1.00
Sum cations	18.91	18.88	18.96
OH	3.09	3.72	3.65
F	0.10	0.28	0.35
Sum OH+F	3.19	4.00	4.00

Notes: R6b = Erzgebirge; Domai = Dora Maira; Laci = Lago di Cignana. Average of 6 EMP analyses for R6b, 8 EMP analyses for Domai, and 15 EMP analyses for Laci. (1) B_2O_3 calculated as B = 3.00 apfu (see text). (2) H_2O content was calculated as OH+F = 4 pfu, except for sample R6b. Total Mn and Fe calculated as MnO and FeO. Chlorine was below the detection limit in all samples. A component was not considered significant unless its value exceeds the uncertainty. b.d. = below detection limit.

* H_2O SIMS data from Marschall et al. (2009).

Z-site occupancy. Because of the enlarged <Z-O> bond-length distances relative to tourmaline with only Al at the Z site having <Z-O> distances of 1.906 ± 0.004 Å (Donnay and Barton 1972; Burns et al. 1994; Hughes et al. 2000; Ertl et al. 2003b, 2005, 2006, 2008b), some Al must be substituted by cations with larger ionic radii. Releasing the Z-site occupancy of the structure refinements did not give evidence for a substitution of Al by Fe^{3+} because the refined occupancy (within a 3σ error) shows only Al (and Mg) at the Z site. However, we cannot exclude that small amounts of Fe^{3+} occupy the Z site. Considering the results of crystal-chemical investigations on the schorl-dravite series by Bloodaxe et al. (1999) and Bosi and Lucchesi (2004) and based on our results with <Z-O> distances (1.926–1.929 Å; Table 3), 0.9–1.0 apfu Mg was assigned to occupy the Z site of all investigated samples.

T-site occupancy. Boron was not measured directly and there is no compelling evidence to suggest substitution of Si by B (within a 3σ error) on the T site. The <T-O> distances (~1.620 Å; Table 3) derived for all three studied samples, do not indicate

any significant (>2% site occupancy) substitution of Si by Al or B (Foit and Rosenberg 1979; MacDonald and Hawthorne 1995; Ertl et al. 1997, 2001, 2005, 2006, 2008b). The very small amounts of Al (≤0.04 apfu), which were assigned to the T site, may be the result of uncertainty in the chemical analyses or normalization procedures (Table 4), and are not verified by single-crystal X-ray data.

V-site and W-site occupation. Ertl et al. (2002) showed that the bond-angle distortion (σ^2_{oct}) of the ZO_6 octahedron in a tourmaline is largely a function of the <Y-O> distance of the respective tourmaline, although the V-site occupant also affects that distortion. The covariance *r*, of <Y-O> and σ^2_{oct} of the ZO_6 octahedron is –0.99 for all investigated tourmaline of Ertl et al. (2002) and Hughes et al. (2004) that are occupied by 3 (OH) groups. The investigated UHP tourmaline samples lie on the V site = 3 (OH) line (see Fig. 3 of Ertl et al. 2002). It is, however, only possible to get a semi-quantitative estimate of the OH content of the O3 site using this relationship. Hence, we assume that the V site in all investigated samples is filled by ~3.0 (OH), which is in contrast to buergerite and "oxy-rossmanite," containing significant amounts of oxygen at this site (Dyar et al. 1998; Ertl et al. 2005). The W site of the investigated tourmaline samples contains low to moderate amounts of F (0.10–0.35 apfu; Table 4). H_2O data, obtained from SIMS analysis, are available for tourmaline from Erzgebirge (sample R6b) from the same hand specimen (Marschall et al. 2009). Therefore, the complete W-site occupancy is estimated to be ~$[O_{0.8}F_{0.1}(OH)_{0.1}]$. The other two samples from Dora Maira and Lago di Cignana exhibit higher F contents, hence the OH content was calculated as 4 – F = OH. With this assumption the calculated H_2O contents result in analytical total sums very close to 100% and are an indication that these values are a good approximation to the actual OH contents.

Because the <T-O> distance is ~1.620 Å for all samples (Table 3), which is a typical bond-length for tourmaline where the T site is almost completely occupied by Si (MacDonald and Hawthorne 1995; Bloodaxe et al. 1999; Ertl et al. 2001; Bosi and Lucchesi 2004, average value for all samples with Si ≥ 5.95 apfu), the following structural formulae were calculated by assuming B = 3 apfu and on the basis of (O,OH,F) = 31 (Table 4):

Dora Maira: $^{X}(Na_{0.90}Ca_{0.05}K_{0.01}\square_{0.04})^{Y}(Mg_{1.78}Al_{0.99}Fe^{2+}_{0.12}Ti^{4+}_{0.03}\square_{0.08})^{Z}(Al_{5.10}Mg_{0.90})(BO_3)_3{}^{T}Si_{6.00}O_{18}{}^{V}(OH)_3{}^{W}[(OH)_{0.72}F_{0.28}]$

Lago di Cignana: $^{X}(Na_{0.84}Ca_{0.09}K_{0.01}\square_{0.06})^{Y}(Mg_{1.64}Al_{0.79}Fe^{2+}_{0.48}Mn^{2+}_{0.06}Ti^{4+}_{0.02}Ni_{0.02}Zn_{0.01})^{Z}(Al_{5.00}Mg_{1.00})(BO_3)_3{}^{T}(Si_{5.98}Al_{0.02})O_{18}{}^{V}(OH)_3{}^{W}[(OH)_{0.65}F_{0.35}]$

Erzgebirge: $^{X}(Na_{0.86}Ca_{0.02}K_{0.02}\square_{0.10})^{Y}(Al_{1.63}Fe^{2+}_{1.23}Ti^{4+}_{0.11}Mg_{0.03}Zn_{0.01})^{Z}(Al_{5.05}Mg_{0.95})(BO_3)_3{}^{T}(Si_{5.96}Al_{0.04})O_{18}{}^{V}(OH)_3{}^{W}[O_{0.81}F_{0.10}(OH)_{0.09}]$.

DISCUSSION

There is a very good positive correlation ($r^2 = 0.99$) between the average charge of the X-site occupants and the F content of the investigated UHP tourmaline samples (Fig. 3). A similar correlation was described for tourmaline of the "fluor-elbaite"-rossmanite solid solution (Ertl et al. 2009). Dutrow and Henry (2000) found a strong negative correlation between the X-site vacancy and the F content in all generations of magmatic to hydrothermal tourmaline from the Cruzeiro Mine, Minas Gerais, Brazil. Henry (2005) evaluated ~600 chemical analyses of different tourmaline varieties in which those with more than 0.5 X-site vacancies had little to no F present. Both relations, using the X-site vacancies or using the average charge of the X-site occupants, are very similar, but the latter approach might be more advantageous. This has been suggested by Ertl et al. (2009), who found that there is a better correlation between the F content and average charge of the X-site occupants than between F and the X-site vacancies.

Henry and Dutrow (1996) pointed out that, in metamorphic tourmaline from pelitic and quartzitic protoliths, the X-site vacancies decrease from 0.6 ±0.2 to 0.30 ±0.05 as temperature increases from 200 to 650 °C with further decrease to 0.05 ±0.05 above 750 °C. In the UHP tourmaline samples, the X-site charges exhibit a negative correlation with temperature of tourmaline formation ($r^2 = 0.92$; Fig. 4). A possible explanation might be a different trend (no increasing $^{[4]}$Al by increasing temperature) of the T-site occupation in UHP tourmaline relative to low-medium pressure tourmaline. Whereas Henry and Dutrow (1996) found that tourmaline of metapelites and metaquartzites that did not exceed metamorphic temperatures of 450 °C contain little or no $^{[4]}$Al, in high-*T* rocks (with $T > 750$ °C), $^{[4]}$Al progressively increases up to an average of 0.25 apfu. In the investigated UHP tourmaline samples that crystallized at temperatures up to ~870 °C, there are no indications for significant amounts of $^{[4]}$Al present; a substitution of Si by Al would increase the size of the tetrahedron. At UHP conditions, it is likely that this replacement does not occur, even at relatively high temperatures. Because F is coupled with the average charge of the X-site occupants (Fig. 3), the F content of the UHP tourmaline shows a good nega-

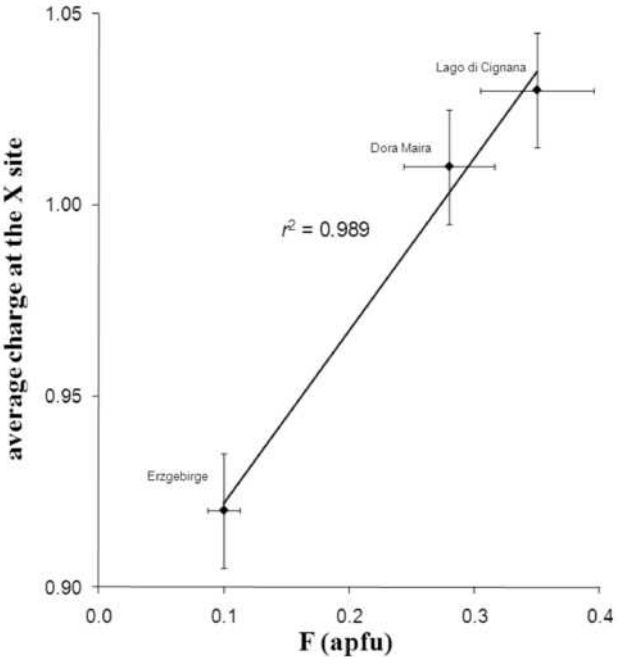

FIGURE 3. Relationship between the F content (Table 4) and average charge at the X site. Bars = average standard deviation (±1σ).

tive correlation (r^2 = 0.97) with the temperature of tourmaline formation (Fig. 5).

Interestingly, a very good correlation (r^2 = 1.00; Fig. 6) exists between the average charge of the X-site occupants and <Y-O> distances (Table 3). The correlation can only be explained by increased $^{Y}Al^{3+}$ content as <Y-O> distances decrease. This is essentially charge-balanced by decreasing local charge at the X site. Another excellent negative correlation was found between the F content and the $^{Y}Al^{3+}$ content (r^2 = 1.00; Fig. 7). This correlation could be explained with the exchange vector $^{Y}AlO(R^{2+}F)_{-1}$. This is consistent with the W site (occupied either by F, O, or OH), being part of the YO_6-polyhedron, and its influence on the observed Al-Mg disorder between the Y and Z sites. There is also a strong negative correlation (r^2 = 0.94) between the <Y-O> distance and the temperature conditions of tourmaline formation (Fig. 8). This correlation suggests an increase in ^{Y}Al content with increasing temperature. Hence, the observed Al-Mg disorder between the Y and Z sites is possibly indirectly dependent on the crystallization temperature. It is interesting to note that the black-colored, Fe-rich, and Mg-bearing tourmaline from Erzgebirge with the formula $^{X}(Na_{0.86}Ca_{0.02}K_{0.02}\square_{0.10})^{Y}(Al_{1.63}Fe^{2+}_{1.23}Ti^{4+}_{0.11}Mg_{0.03}Zn_{0.01})^{Z}(Al_{5.05}Mg_{0.95})(BO_3)_3{}^{T}(Si_{5.96}Al_{0.04})O_{18}{}^{V}(OH)_3$

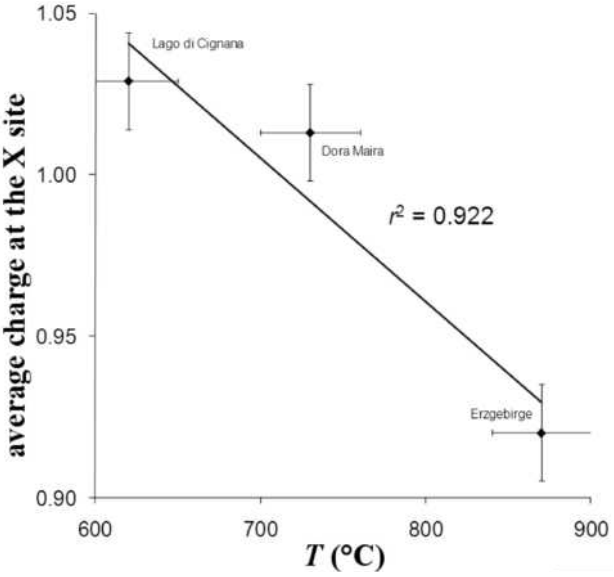

FIGURE 4. Relationship between the average charge at the X site and the temperature conditions of tourmaline formation. Bars = average estimated standard deviation (±1σ).

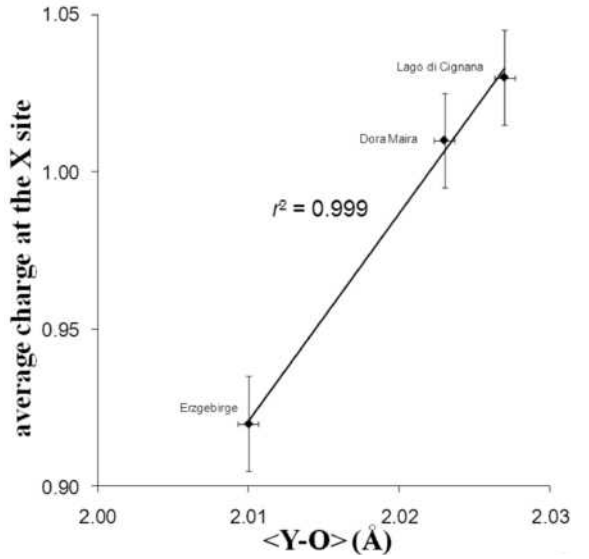

FIGURE 6. Relationship between the average charge at the X site and the <Y-O> distance (Table 3). Bars = average estimated standard deviation (±1σ).

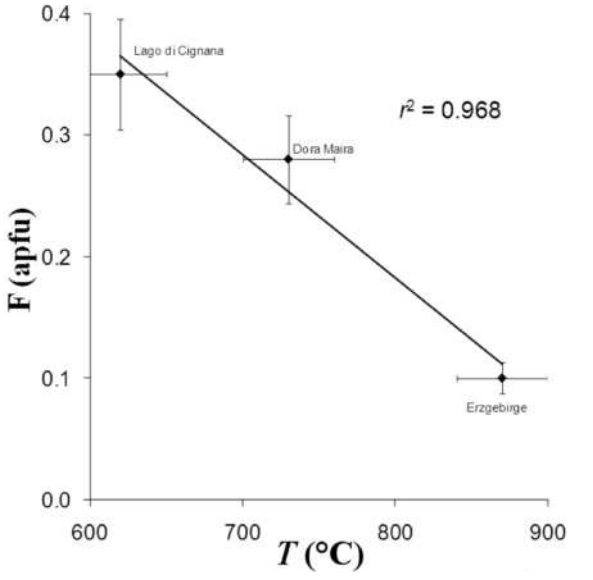

FIGURE 5. Relationship between the F content (Table 4) and the temperature conditions of tourmaline formation. By using the refined F data (Table 2) the correlation coefficient becomes r^2 = 1.000. Bars = average estimated standard deviation (±1σ).

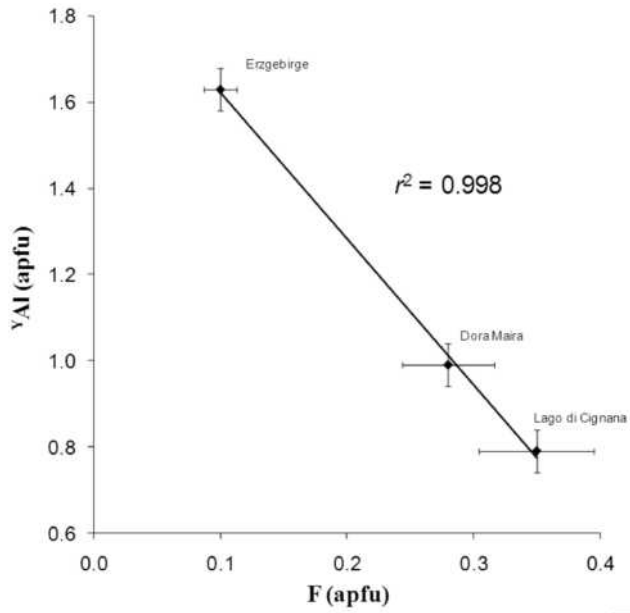

FIGURE 7. Relationship between F content (Table 4) and the Al content of the Y site. Bars = average estimated standard deviation (±1σ).

$^{W}[O_{0.81}F_{0.10}(OH)_{0.09}]$ is dominated by Al at the Y site.

There is an excellent positive correlation ($r^2 = 0.99$) between the $^{[6]}$Al content (sum of Al at the Y and Z site) of the investigated UHP tourmaline samples and the temperature of tourmaline formation (Figs. 9 and 10). An increase of octahedral Al in the UHP tourmaline samples can be explained via a combination of the (simplified) exchange vectors $^{X}\square\,^{[6]}AlOH(NaR^{2+}F)_{-1}$, $^{[6]}AlO(R^{2+}F)_{-1}$, and $^{X}\square\,^{[6]}AlOH(CaR^{2+}O)_{-1}$ (with R^{2+} = Fe^{2+} + Mn^{2+} + Mg), in which the first vector is a modified version of the exchange vector suggested by Henry and Dutrow (1996), $^{X}\square\,Al(NaR^{2+})_{-1}$, for diagenetic to high-grade metamorphic tourmaline.

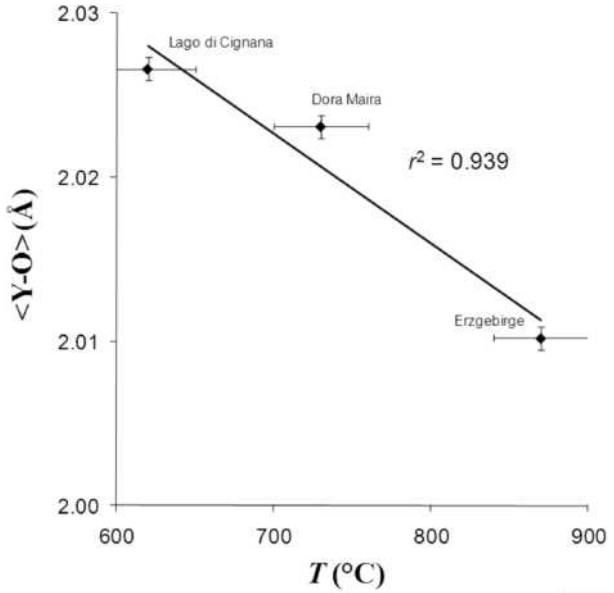

FIGURE 8. Relationship between the <Y-O> distance and the temperature conditions of tourmaline formation. Vertical bars = average estimated standard deviation (±1σ).

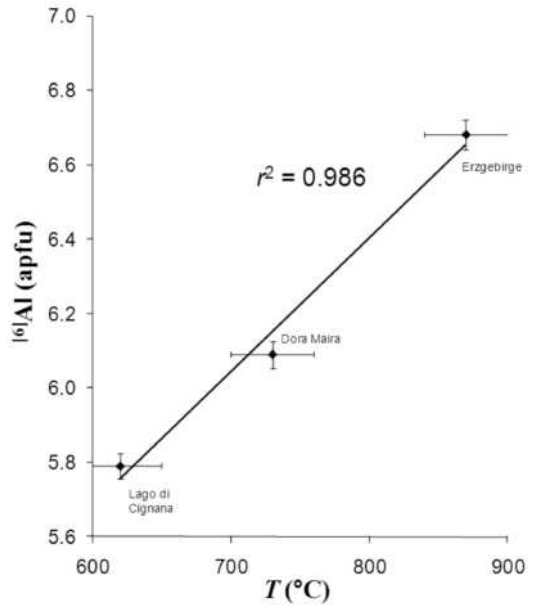

FIGURE 9. Relationship between the $^{[6]}$Al content (sum of Al at the Y- and Z sites) and the temperature conditions of tourmaline formation. Vertical bars = average estimated standard deviation (±1σ).

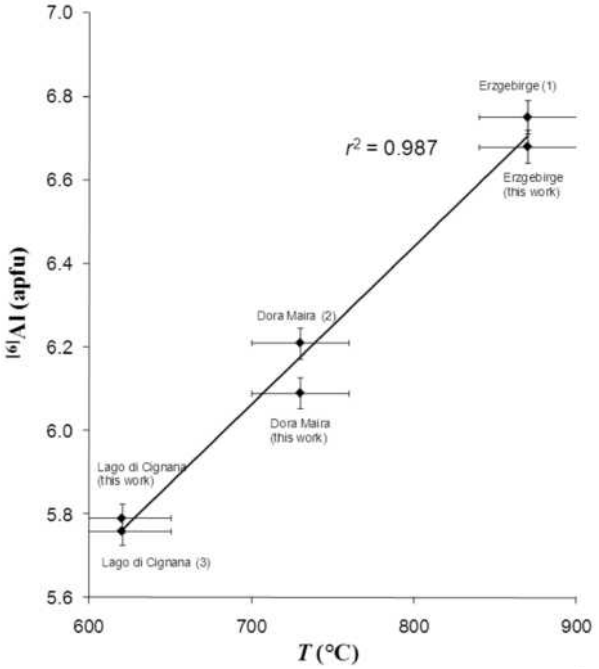

FIGURE 10. Relationship between the temperature conditions of tourmaline formation and the $^{[6]}$Al content (sum of Al at the Y and Z sites). Also plotted are data from samples R6b (1) coesite-bearing mantle of the tourmaline, Erzgebirge, Germany (Marschall et al. 2009), (2) dravite inclusion from a small pyrope crystal from Dora Maira (Schreyer 1985), and (3) a tourmaline from Lago di Cignana, Zermatt-Saas zone, Western Alps (Reinecke 1991). Vertical bars = average estimated standard deviation (1σ).

Tourmaline crystals from UHP metamorphic conditions are uncommon. Further studies should now focus on the interrelation between the crystal chemistry and metamorphic *P-T* conditions of tourmaline by investigating samples of well-defined metamorphic histories, including high-*P* and diagenetic to high-*T* samples. Consequently, further detailed field, petrographic, and experimental studies undoubtedly would help to solve the problems associated with the tourmaline chemistry (including the occupancy of the Y and Z site) in metamorphic terranes.

ACKNOWLEDGMENTS

Special thanks to Thomas Reinecke, Bochum, Germany, for providing samples of the tourmaline- and piemontite-bearing garnet-phengite-coesite-schist from Lago di Cignana, Western Alps, as well as for the photograph of the euhedral tourmaline crystal with the coesite inclusion, for different references and for helpful discussions. We thank A. Wagner, Vienna, Austria, for preparing the tourmaline samples and Olaf Medenbach for extracting pieces of the tourmaline from a Dora Maira thin section. This work was supported by Österreichischer Fonds zur Förderung der wissenschaftlichen Forschung (FWF) project no. P20509. We sincerely thank Alfonso Pesquera and Carl Francis for their careful reviews of the manuscript.

REFERENCES CITED

Bebout, G.E. and Nakamura, E. (2003) Record in metamorphic tourmaline of subduction-zone devolatilization and boron cycling. Geology, 31, 407–410.

Bernardelli, P., Castelli, D., and Rossetti, P. (2000) Tourmaline-rich ore-bearing hydrothermal system of lower Valle del Cervo (western Alps, Italy): Field relationships and petrology. Schweizerische Mineralogische und Petrographische Mitteilungen, 80, 257–277.

Bloodaxe, E.S., Hughes, J.M., Dyar, M.D., Grew, E.S., and Guidotti, C.V. (1999) Linking structure and chemistry in the schorl-dravite series. American Min-

eralogist, 84, 922–928.
Bohlen, S.R. and Boettcher, A.L. (1982) The quartz-coesite transformation: A pressure determination and the effects of other components. Journal of Geophysical Research, 87, 7073–7078.
Bosi, F. and Lucchesi, S. (2004) Crystal chemistry of the schorl-dravite series. European Journal of Mineralogy, 16, 335–344.
Bosi, F., Lucchesi, S., and Reznitskii, L. (2004) Crystal chemistry of the dravite-chromdravite series. European Journal of Mineralogy, 16, 345–352.
Bruker (2001) SaintPlus. Bruker AXS Inc., Madison, Wisconsin.
Bundy, F.P. (1980) The *P*,*T* phase and reaction diagram for elemental carbon. Journal of Geophysical Research, 88, 6930–6936.
Burns, P.C., MacDonald, D.J., and Hawthorne, F.C. (1994) The crystal chemistry of manganese-bearing elbaite. Canadian Mineralogist, 32, 31–41.
Chopin, C. (1984) Coesite and pure pyrope in high-grade blueschists of the Western Alps: a first record and some consequences. Contributions to Mineralogy and Petrology, 86, 107–118.
Compagnoni, R. (2003) HP metamorphic belt of the western Alps. Episodes, 26, 200–204.
Deer, W.A., Howie, R.A., and Zussman, J. (1992) An Introduction to the Rock-Forming Minerals, 2nd edition, 712 p. Longman, London.
Dobretsov, N.L., Sobolev, N.V., Shatsky, V.S., Coleman, R.G., and Ernst, W.G. (1995) Geotectonic evolution of diamondiferous paragneisses of the Kokchetav complex, Northern Kazakhstan—the geologic enigma of ultrahigh-pressure crustal rocks within Phanerozoic foldbelt. The Island Arc, 4, 267–279.
Donnay, G. and Barton Jr., P. (1972) Refinement of the crystal structure of elbaite and the mechanism of tourmaline solid solution. Tschermaks Mineralogisch Petrographische Mitteilungen, 18, 273–286.
Dutrow, B. and Henry, D.J. (2000) Complexly zoned fibrous tourmaline, Cruzeiro mine, Minas Gerais, Brazil: A record of evolving magmatic and hydrothermal fluids. Canadian Mineralogist, 38, 131–143.
Dutrow, B., Foster Jr., C.T., and Henry, D.J. (1999) Tourmaline-rich pseudomorphs in sillimanite zone metapelites: Demarcation of an infiltration front. American Mineralogist, 84, 794–805.
Dyar, M.D., Taylor, M.E., Lutz, T.M., Francis, C.A., Guidotti, C.V., and Wise, M. (1998) Inclusive chemical characterization of tourmaline: Mössbauer study of Fe valence and site occupancy. American Mineralogist, 83, 848–864.
Ertl, A., Pertlik, F., and Bernhardt, H.-J. (1997) Investigations on olenite with excess boron from the Koralpe, Styria, Austria. Österreichische Akademie der Wissenschaften, Mathematisch-Naturwissenschaftliche Klasse, Abteilung I, Anzeiger, 134, 3–10.
Ertl, A., Hughes, J.M., and Marler, B. (2001) Empirical formulae for the calculation of <*T*-O> and *X*-O2 bond lengths in tourmaline and relations to tetrahedrally-coordinated boron. Neues Jahrbuch für Mineralogie, Monatshefte, 12, 548–557.
Ertl, A., Hughes, J.M., Pertlik, F., Foit Jr., F.F., Wright, S.E., Brandstätter, F., and Marler, B. (2002) Polyhedron distortions in tourmaline. Canadian Mineralogist, 40, 153–162.
Ertl, A., Hughes, J.M., Brandstätter, F., Dyar, M.D., and Prasad, P.S.R. (2003a) Disordered Mg-bearing olenite from a granitic pegmatite from Goslarn, Austria: A chemical, structural, and infrared spectroscopic study. Canadian Mineralogist, 41, 1363–1370.
Ertl, A., Hughes, J.M., Prowatke, S., Rossman, G.R., London, D., and Fritz, E.A. (2003b) Mn-rich tourmaline from Austria: structure, chemistry, optical spectra, and relations to synthetic solid solutions. American Mineralogist, 88, 1369–1376.
Ertl, A., Rossman, G.R., Hughes, J.M., Prowatke, S., and Ludwig, T. (2005) Mn-bearing "oxy-rossmanite" with tetrahedrally coordinated Al and B from Austria: Structure, chemistry, and infrared and optical spectroscopic study. American Mineralogist, 90, 481–487.
Ertl, A., Hughes, J.M., Prowatke, S., Ludwig, T., Prasad, P.S.R., Brandstätter, F., Körner, W., Schuster, R., Pertlik, F., and Marschall, H. (2006) Tetrahedrally coordinated boron in tourmalines from the liddicoatite-elbaite series from Madagascar: Structure, chemistry, and infrared spectroscopic studies. American Mineralogist, 91, 1847–1856.
Ertl, A., Rossman, G.R., Hughes, J.M., Ma, C., and Brandstätter, F. (2008a) V^{3+}-bearing, Mg-rich, strongly disordered olenite from a graphite deposit near Amstall, Lower Austria: A structural, chemical and spectroscopic investigation. Neues Jahrbuch für Mineralogie, Monatshefte Abhandlungen, 184, 243–253.
Ertl, A., Tillmanns, E., Ntaflos, T., Francis, C., Giester, G., Körner, W., Hughes, J.M., Lengauer, C., and Prem, M. (2008b) Tetrahedrally coordinated boron in Al-rich tourmaline and its relationship to the pressure–temperature conditions of formation. European Journal of Mineralogy, 20, 881–888.
Ertl, A., Kolitsch, U., Meyer, H.-P., Ludwig, T., Lengauer, C.L., Nasdala, L., and Tillmanns, E. (2009) Substitution mechanism in tourmalines of the "fluor-elbaite"-rossmanite series from Wolkenburg, Saxony, Germany. Neues Jahrbuch für Mineralogie, Monatshefte Abhandlungen, 186, 51–61.
Fischer, R.X. and Tillmanns, E. (1988) The equivalent isotropic displacement factor. Acta Crystallographica, C44, 775–776.
Foit Jr., F.F. and Rosenberg, P.E. (1979) The structure of vanadium-bearing tourmaline and its implications regarding tourmaline solid solutions. American Mineralogist, 64, 788–798.
Grice, J.D. and Ercit, T.S. (1993) Ordering of Fe and Mg in the tourmaline crystal structure: the correct formula. Neues Jahrbuch für Mineralogie, Monatshefte Abhandlungen, 165, 245–266.
Hawthorne, F.C. and Henry, D.J. (1999) Classification of the minerals of the tourmaline group. European Journal of Mineralogy, 11, 201–215.
Hawthorne, F.C., MacDonald, D.J., and Burns, P.C. (1993) Reassignment of cation site-occupancies in tourmaline: Al-Mg disorder in the crystal structure of dravite. American Mineralogist, 78, 265–270.
Henry, D.J. (2005) Fluorine—X-site vacancy avoidance in natural tourmaline: Internal vs. external control. 2005 Goldschmidt Conference, May 20–25, Moscow, Idaho, Abstracts Volume, abstract no. 1318.
Henry, D.J. and Dutrow, B.L. (1992) Tourmaline in a low grade clastic metasedimentary rocks: an example of the petrogenetic potential of tourmaline. Contributions to Mineralogy and Petrology, 112, 203–218.
——— (1996) Metamorphic tourmaline and its petrologic applications. In E.S. Grew and L.M. Anovitz, Eds., Boron: Mineralogy, Petrology, and Geochemistry, 33, p. 503–557. Reviews in Mineralogy and Geochemistry, Mineralogical Society of America, Chantilly, Virginia.
Henry, D.J. and Guidotti, C.V. (1985) Tourmaline in the staurolite grade metapelites of NW Maine: a petrogenetic indicator mineral. American Mineralogist, 70, 1–15.
Henry, D.J., Kirkland, B.L., and Kirkland, D.W. (1999) Sector-zoned tourmaline from the cap rock of a salt dome. European Journal of Mineralogy, 11, 263–280.
Henry, D.J., Sun, H., Slack, J., and Dutrow, B.L. (2008) Tourmaline in meta-evaporites and highly magnesian rocks: perspectives from Namibian tourmalinites. European Journal of Mineralogy, 20, 973–993.
Hermann, J. (2003) Experimental evidence for diamond-facies metamorphism in the Dora-Maira massif. Lithos, 70, 163–182.
Hughes, J.M., Ertl, A., Dyar, M.D., Grew, E.S., Shearer, C.K., Yates, M.G., and Guidotti, C.V. (2000) Tetrahedrally coordinated boron in a tourmaline: boron-rich olenite from Stoffhütte, Koralpe, Austria. Canadian Mineralogist, 38, 861–868.
Hughes, J.M., Ertl, A., Dyar, M.D., Grew, E.S., Wiedenbeck, M., and Brandstätter, F. (2004) Structural and chemical response to varying $^{[4]}$B content in zoned Fe-bearing olenite from Koralpe, Austria. American Mineralogist, 89, 447–454.
Kawakami, T. (2001) Tourmaline breakdown in the migmatite zone of the Ryoke metamorphic belt, SW Japan. Journal of Metamorphic Geology, 19, 61–75.
Krosse, S. (1995) Hochdrucksynthese, stabilität und eigenschaften der borsilikate dravit und kornerupin sowie darstellung und stabilitätsverhalten eines neuen Mg-Al-borates. Ph.D. thesis, Ruhr-Universität Bochum, Germany.
Kretz, R. (1983) Symbols for rock-forming minerals. American Mineralogist, 68, 277–279.
MacDonald, D.J. and Hawthorne, F.C. (1995) The crystal chemistry of Si ↔ Al substitution in tourmaline. Canadian Mineralogist, 33, 849–858.
Manning, D.A.C. and Pichavant, M. (1983) The role of fluorine and boron in the generation of granitic melts. In M.P. Atherton and C.D. Gribble, Eds., Migmatites, Melting, and Metamorphism, Chapter 7, p. 94–109. Shiva Publications, Cheshire.
Marschall, H.R., Ertl, A., Hughes, J.M., and McCammon, C. (2004) Metamorphic Na- and OH-rich disordered dravite with tetrahedral boron, associated with omphacite, from Syros, Greece: chemistry and structure. European Journal of Mineralogy, 16, 817–823.
Marschall, H.R., Korsakov, A.V., Luvizotto, G.L., Nasdala, L., and Ludwig, T. (2009) On the occurrence and boron isotopic composition of tourmaline in (ultra)high-pressure metamorphic rocks. Journal of the Geological Society, 166, 811–823.
Massonne, H.J. (2003) A comparison of the evolution of diamondiferous quartz-rich rocks from the Saxonian Erzgebirge and the Kokchetav massif: are so-called diamondiferous gneisses magmatic rocks? Earth and Planetary Science Letters, 216, 347–364.
Massonne, H.J., Kennedy, A., Nasdala, L., and Theye, T. (2007) Dating of zircon and monazite from diamondiferous quartzofeldspathic rocks of the Saxonian Erzgebirge—hints at burial and exhumation velocities. Mineralogical Magazine, 71, 407–425.
Ota, T., Kobayashi, K., Katsura, T., and Nakamura, E. (2008) Tourmaline breakdown in a pelitic system: Implications for boron cycling through subduction zones. Contributions to Mineralogy and Petrology, 155, 19–32.
Reinecke, T. (1991) Very-high-pressure metamorphism and uplift of coesite-bearing metasediments from the Zermatt-Saas zone, Western Alps. European Journal of Mineralogy, 3, 7–17.
——— (1998) Prograde high- to ultrahigh-pressure metamorphism and exhumation of oceanic sediments at Lago di Cignana, Zermatt-Saas Zone, western Alps. Lithos, 42, 147–189.
Reinitz, I.L. and Rossman, G.R. (1988) Role of natural radiation in tourmaline coloration. American Mineralogist, 73, 822–825.
Robbins, C.R. and Yoder Jr., H.S. (1962) Stability relations of dravite, a tourmaline. Carnegie Institution of Washington Yearbook, 61, 106–108.

Rossman, G.R. (2008) Colors in minerals caused by intervalence charge transfer (IVCT). California Institute of Technology Pasadena, California, http://minerals.gps.caltech.edu/COLOR_Causes/IVCT/index.htm (accessed 12-18-2008).

Rötzler, K., Schumacher, R., Maresch, W.V., and Willner, A.P. (1998) Characterization and geodynamic implications of contrasting metamorphic evolution in juxtaposed high-pressure units of the western Erzgebirge (Saxony, Germany). European Journal of Mineralogy, 10, 261–280.

Schertl, H.-P. and Schreyer, W. (2008) Geochemistry of coesite-bearing "pyrope quartzite" and related rocks from the Dora Maira Massif, Western Alps. European Journal of Mineralogy, 20, 791–809.

Schertl, H.P., Schreyer, W., and Chopin, C. (1991) The pyrope-coesite rocks and their country rocks at Parigi, Dora Maira Massif, Western Alps: detailed petrography, mineral chemistry and *P-T* path. Contributions to Mineralogy and Petrology, 108, 1–21.

Schmädicke, E. and Müller, W.F. (2000) Unusual exsolution phenomena in omphacite and partial replacement of phengite by phlogopite plus kyanite in an eclogite from the Erzgebirge. Contributions to Mineralogy and Petrology, 139, 629–642.

Schreyer, W. (1985) Metamorphism of crustal rocks at mantle depth: High pressure minerals and mineral assemblages in metapelites. Fortschritte der Mineralogie, 63, 227–261.

Sengupta, N., Mukhopadhyay, D., Sengupta, P., and Hoffbauer, R. (2005) Tourmaline-bearing rocks in the Singhbhum shear zone, eastern India: Evidence of boron infiltration during regional metamorphism. American Mineralogist, 90, 1241–1255.

Sheldrick, G.M. (1997) SHELXL-97, a program for crystal structure refinement. University of Göttingen, Germany.

Slack, J.F. (1996) Tourmaline associations with hydrothermal ore deposits. In E.S. Grew and L.M. Anovitz, Eds., Boron: Mineralogy, Petrology, and Geochemistry, 33, p. 559–644. Reviews in Minerology, Mineralogical Society of America, Chantilly, Virginia.

Thomson, J.A. (2006) A rare garnet-tourmaline-sillimanite-biotite-ilmenite-quartz assemblage from the granulite facies of south-central Massachusetts. American Mineralogist, 91, 1730–1738.

Trumbull, R.B., Krienitz, M.S., Gottesmann, B., and Wiedenbeck, M. (2008) Chemical and boron-isotope variations in tourmalines from an S-type granite and its source rocks: the Erongo granite and tourmalinites in the Damara Belt, Namibia. Contributions to Mineralogy and Petrology, 155, 1–18.

van den Bleeken, G., Corteel, C., and van den Haute, P. (2007) Epigenetic to low-grade tourmaline in the Gdoumont metaconglomerates (Belgium): A sensitive probe of its chemical environment of formation. Lithos, 95, 165–176.

van Hinsberg, V.J. and Marschall, H.R. (2007) Boron isotope and light element sector zoning in tourmaline: Implications for the formation of B-isotopic signatures. Chemical Geology, 238, 141–148.

van Hinsberg, V.J. and Schumacher, J.C. (2007) Intersector element partitioning in tourmaline: a potentially powerful single crystal thermometer. Contributions to Mineralogy and Petrology, 153, 289–301.

von Goerne, G., Franz, G., and Heinrich, W. (2001) Synthesis of tourmaline solid solutions in the system Na_2O-MgO-Al_2O_3-SiO_2-B_2O_3-H_2O-HCl and the distribution of Na between tourmaline and fluid at 300 to 700 °C and 200 MPa. Contributions to Mineralogy and Petrology, 141, 160–173.

Werding, G. and Schreyer, W. (2002) Experimental studies on borosilicates and selected borates. In E.S. Grew and L.M. Anovitz, Eds., Boron: Mineralogy, Petrology and Geochemistry, 33, p. 117–163. Reviews in Mineralogy, Mineralogical Society of America, Chantilly, Virginia.

Willner, A.P., Rötzler, K., and Maresch, W.V. (1997) Pressure-temperature and fluid evolution of quartzo-feldspathic metamorphic rocks with a relic high-pressure, granulite-facies history from the Central Erzgebirge (Saxony, Germany). Journal of Petrology, 38, 307–336.

MANUSCRIPT RECEIVED MAY 7, 2009
MANUSCRIPT ACCEPTED AUGUST 13, 2009
MANUSCRIPT HANDLED BY M. DARBY DYAR